Analyzing Impact of BESS Allocation on Hosting Capacity in Distribution Networks

Naihao Shi, Rui Cheng, Qianzhi Zhang, Zhaoyu Wang
Department of Electrical and Computer Engineering
Iowa State University
Ames, IA, USA
snh0812@iastate.edu, ruicheng@iastate.edu, qianzhi@iastate.edu, wzy@iastate.edu

2022 North American Power Symposium (NAPS) | 978-1-6654-9921-7/22/$31.00 ©2022 IEEE | DOI: 10.1109/NAPS56150.2022.10012229

***Abstract*—Given the increasing number of power system reliability problems caused by the high penetration of distributed generation, hosting capacity, which refers to the maximum amount of distributed generation to be accommodated in a power network, is of great importance for power system planning and management. To this end, this paper mainly studies the impact of battery energy storage system (BESS) allocation on hosting capacity in distribution systems. Two types of BESS allocation are considered, i.e., the centralized BESS allocation and the distributed BESS allocation. With respect to the centralized BESS allocation, a large BESS is installed near the feeder head to evaluate the hosting capacity. In contrast, with respect to the distributed BESS allocation, a series of small BESSs are distributed across the distribution network to evaluate the hosting capacity, where the locations and operation status of those small BESSs are determined by the mixed-integer program. Finally, the performance of centralized and distributed BESS allocations is tested on the IEEE 123-bus test system and the results show that installing BESS can greatly increase the system's maximum hosting capacity. Compared with the centralized BESS allocation, the distributed allocation of BESSs can further improve the system hosting capacity.**

***Index Terms*—Distributed generation, battery energy storage system (BESS), hosting capacity, BESS allocation**

I. Introduction

Recent years have seen a dramatic surge of renewable energy generation, e.g., photovoltaics (PV) and wind power resources [1], paving the way to a future carbon-free energy architecture. However, it also poses new challenges to power system planning, management and operation. To estimate the network's capacity to accommodate renewable energy resources without affecting the power system security and stability and provide some instructions for future planning and management, the concept of hosting capacity has been put forward. Hosting capacity is normally defined as the maximum capacity of distributed generation that can be installed to a network without causing any operating constraint violations [2].

The main factors and indices, limiting the hosting capacity, include power quality, feeder's thermal constraints, and the reverse power flow limits or voltage limits [3]. Based on these factors and indices, different methods have been proposed to estimate and improve hosting capacity. Generally speaking, those methods can be classified into two types, i.e., simulation-based approaches and optimization-based approaches. With respect to simulation-based approaches, it can be summarized as iteratively increasing the penetration level of distributed generation until the selected system operation index gets beyond the safety range. For example, in [2], the maximum hosting capacity is estimated by repetitively computing the power flow with an increasing penetration of renewable energy. Compared to simulation-based approaches, optimization-based approaches formulate hosting capacity problems as optimization programming problems, which can take full advantage of the network management approaches like voltage/VAr control, battery energy storage system (BESS) operation and network reconfiguration to enhance the system hosting capacity. Voltage/VAr control with PV inverters is considered in [4], [5] to integrate higher penetration levels of renewable energy resources. And [6] focuses on on-load tap changers (OLTCs), power factor control and curtailment of distributed generation. Besides, network reconfiguration is studied in [7] to enhance the hosting capacity. However, the operation of BESSs is not taken into account in [4]–[6].

Considering the intermittent and fluctuant nature of renewable energy resources, BESSs can provide the time-shifting energy supply which makes up the time-varying characteristics of renewable energy generation, thus enabling the larger hosting capacity to be accommodated to the power system. BESSs have been widely studied in various research fields, e.g., [8]. In [9], [10], one single BESS is installed at a certain bus (near one of the wind farms [9] or near the feeder head [10]) in the distributed network to improve the hosting capacity. The optimal placement of one single BESS is formulated as an optimization problem in [11]. Since renewable energy resources are often distributed at different locations across the distribution network, the allocation of multiple BESSs should be considered. In [12], multiple BESSs are allocated to several candidate buses to minimize the power unbalance, which can increase the system hosting capacity at the same time. In [9]–[12], the impact of BESSs on the system hosting capacity is more or less discussed. However, they do not study how different BESS allocations affect the system hosting capacity

This work was supported by the U.S. Department of Energy Wind Energy Technologies Office under Grant DE-EE0008956, the National Science Foundation under Grant ECCS 1929975, and the U.S. Department of Energy Advanced Grid Modeling Program under Grant DE-OE0000875.

in detail.

To this end, this paper mainly analyzes the impact of different BESS allocations on the hosting capacity in distribution networks. First, the centralized BESS allocation is applied to a three-phase unbalanced network to test the performance of hosting capacity enhancement on the premise of no reverse power flow and voltage violations. Then, the distributed BESS allocation is utilized to improve the system hosting capacity, where a series of small BESSs are distributed across the distribution network. The locations and operation status of those small BESSs are determined by the mixed-integer program to maximize the system hosting capacity. Finally, the results without BESSs and with different BESS allocations are compared and analyzed. The results show the distributed BESS allocation can achieve the best performance regarding the hosting capacity improvement.

II. Problem Formulation

This section introduces the mathematical formulation of the hosting capacity enhancement problem by optimally allocating the BESSs in unbalanced distribution networks. First, the three-phase linearized power flow model as well as its compact form are introduced. Then, BESS operation constraints are discussed. Finally, the mathematical formulations of centralized and distributed BESS allocations for the hosting capacity problem are provided in detail.

A. Three-phase Linearized Power Flow Model

When calculating the hosting capacity, it is important to satisfy the system operation limits, which are typically presented by the power flow.

Consider a radial three-phase unbalanced network containing $n+1$ buses and let set $\{0\}\bigcup\mathcal{N}$ represent the index of all the buses, where $\{0\}$ denotes the swing bus and set $\mathcal{N}=\{1,...,n\}$ denotes all other buses. For any bus $j\in\{0\}\bigcup\mathcal{N}$, $\mathcal{N}_j$ is the set of all children buses of bus j. The set consisting all line segments in the distribution network can be expressed as: $\mathcal{L}=\{\ell_j=(i,j)|i=m(j),j\in\mathcal{N}\}$, where $m(j)$ denotes the parent bus of bus j. Let column vectors $\boldsymbol{v}_i(t)=[v_{i,\phi}(t)]_{\phi\in\{a,b,c\}}$, $\boldsymbol{p}_i(t)=[p_{i,\phi}(t)]_{\phi\in\{a,b,c\}}$ and $\boldsymbol{q}_i(t)=[q_{i,\phi}(t)]_{\phi\in\{a,b,c\}}$ collect the three-phase squared voltage magnitudes, net active and reactive power consumption for bus i at time t, respectively. And let column vectors $\boldsymbol{P}_{ij}(t)=[P_{ij,\phi}(t)]_{\phi\in\{a,b,c\}}$ and $\boldsymbol{Q}_{ij}(t)=[Q_{ij,\phi}(t)]_{\phi\in\{a,b,c\}}$ collect the active and reactive power flows in line (i,j) at time t. Without loss of generality,[1] each line segment is assumed to be a 3-phase line segment. The linearized distribution power flow for the three-phase distribution network can be expressed as:

$$\boldsymbol{P}_{ij}(t)=\sum_{k\in\mathcal{N}_j}\boldsymbol{P}_{jk}(t)+\boldsymbol{p}_j(t),\forall\ell_j,t \tag{1a}$$

$$\boldsymbol{Q}_{ij}(t)=\sum_{k\in\mathcal{N}_j}\boldsymbol{Q}_{jk}(t)+\boldsymbol{q}_j(t),\forall\ell_j,t \tag{1b}$$

$$\boldsymbol{v}_i(t)-\boldsymbol{v}_j(t)=2(\bar{\boldsymbol{R}}_{ij}\boldsymbol{P}_{ij}(t)+\bar{\boldsymbol{X}}_{ij}\boldsymbol{Q}_{ij}(t)),\forall\ell_j,t \tag{1c}$$

where $\bar{\boldsymbol{R}}_{ij}$ and $\bar{\boldsymbol{X}}_{ij}$ are 3-phase resistance and reactance matrices (p.u.) for line segment (i,j) after transformation. For ease of notation, the three-phase unbalanced power flow can be further written as a compact form. For the unbalanced radial network with the bus set $\{0\}\bigcup\mathcal{N}$ and the line set $\mathcal{L}$, every bus $j\in\{0\}\bigcup\mathcal{N}$ and every line segment $\ell_j\in\mathcal{L}$ are presented in a three-phase form. The squared voltage magnitudes, the net load consumption and the power flows for the three-phase distribution network are denoted by the following column vectors: $\boldsymbol{v}(t)=[\boldsymbol{v}_i(t)]_{i\in\mathcal{N}}$, $\boldsymbol{p}(t)=[\boldsymbol{p}_i(t)]_{i\in\mathcal{N}}$, $\boldsymbol{q}(t)=[\boldsymbol{q}_i(t)]_{i\in\mathcal{N}}$, $\boldsymbol{P}(t)=[\boldsymbol{P}_{ij}(t)]_{(i,j)\in\mathcal{L}}$ and $\boldsymbol{Q}(t)=[\boldsymbol{Q}_{ij}(t)]_{(i,j)\in\mathcal{L}}$. With all the notations listed above, the three-phase unbalanced power flow in (1) can be compactly expressed as [14]:

$$\boldsymbol{A}\boldsymbol{P}(t)=-\boldsymbol{p}(t) \tag{2a}$$

$$\boldsymbol{A}\boldsymbol{Q}(t)=-\boldsymbol{q}(t) \tag{2b}$$

$$\begin{bmatrix}\boldsymbol{A}_0 & \boldsymbol{A}^T\end{bmatrix}\begin{bmatrix}\boldsymbol{v}_0(t)\\ \boldsymbol{v}(t)\end{bmatrix}=2\Big(\boldsymbol{D}_r\boldsymbol{P}(t)+\boldsymbol{D}_x\boldsymbol{Q}(t)\Big) \tag{2c}$$

where $\bar{\boldsymbol{A}}=[\boldsymbol{A}_0,\boldsymbol{A}^T]^T$ is the incidence matrix for the distribution network. [2] And $\boldsymbol{D}_r$ and $\boldsymbol{D}_x$ are block diagonal matrices:

$$\boldsymbol{D}_r=\text{diag}(\bar{\boldsymbol{R}}_{m(1)1},...,\bar{\boldsymbol{R}}_{m(n)n})$$
$$\boldsymbol{D}_x=\text{diag}(\bar{\boldsymbol{X}}_{m(1)1},...,\bar{\boldsymbol{X}}_{m(n)n})$$

B. BESS Operation Constraints

Integration of BESSs is an efficient way to increase the system hosting capacity since BESSs can provide the time-shifting energy supply which makes up the time-varying characteristics of renewable energy resources. Thus, the BESSs have the great potential to increase the system hosting capacity. Let $\boldsymbol{p}_i^C(t)=[p_{i,\phi}^C(t)]_{\phi\in\{a,b,c\}}$ and $\boldsymbol{p}_i^D(t)=[p_{i,\phi}^D(t)]_{\phi\in\{a,b,c\}}$ denote the three-phase charging and discharging power for the BESS located at bus i, the operation constraints of BESSs are given as:

$$0\le p_{i,\phi}^C(t)\le\overline{p_{i,\phi}^C}\cdot\mu_i(t),\forall i,\phi,t \tag{3a}$$

$$0\le p_{i,\phi}^D(t)\le\eta^D\cdot\overline{p_{i,\phi}^D}\cdot(1-\mu_i(t)),\forall i,\phi,t \tag{3b}$$

$$SoC_i(t)=SoC_i(t-1)+\frac{\eta^C\cdot\sum_\phi p_{i,\phi}^C(t)\cdot\Delta t}{E_i}-\frac{\sum_\phi p_{i,\phi}^D(t)\cdot\Delta t}{\eta^D\cdot E_i},\forall i,\phi,t \tag{3c}$$

$$\underline{SoC}_i\le SoC_i(t)\le\overline{SoC}_i,\forall i,t \tag{3d}$$

[1] As discussed and illustrated in Appendix B of [13], any k-phase line segment with $k<3$ can be represented as a 3-phase line segment by introducing an appropriate number of additional "virtual" circuits for this line segment with "virtual" phases whose self-impedance and mutual impedance are set to zero. The introduction of these virtual elements does not affect the resulting linearized power flow solutions.

[2] A numerical example illustrating the construction of $\bar{\boldsymbol{A}}$ for an unbalanced distribution network is given in Appendix C of [13].

Including the binary variable $\mu_i(t)$ that decides the BESS working status, equations (3a) and (3b) are the charging and discharging power limits of BESS at bus i, time t. When $\mu_i(t)$ is equal to 0 or 1, the BESS works at the discharging mode and charging mode, respectively. Note that $u_i(t)$ is only related to the bus index i. This is because, in practice, all phase units of a multi-phase BESS always work at the same status (charging or discharging). η^D and η^C are the discharging and charging efficiency ratio. The state of charge (SoC) is calculated by equation (3c), where E_i is the capacity of BESS located at bus i and Δt is the time interval (which is set to one hour in this work). Equation (3d) means that the SoC must maintain in a certain range to avoid overcharging or undercharging.

C. Centralized BESS Allocation and Operation

The centralized BESS allocation means to install one large BESS near the feeder head. The goal of this subsection is to maximize the system hosting capacity by operating the charging and discharging of the centralized BESS. The hourly PV outputs can be presented as the installed capacity multiplied by a time-series ratio $s(t)$:

$$p_{i,\phi}^{inv}(t) = S_{i,\phi}^{g} \cdot r(t) \tag{4}$$

In this problem, the PV inverters' ability to provide or absorb reactive power is also considered for hosting capacity enhancement. Then, the net power consumption $\boldsymbol{p}(t)$ and $\boldsymbol{q}(t)$ in the compact power flow form can be represented by the system loads, PV outputs and BESS charging and discharging power:

$$\boldsymbol{p}(t) = \boldsymbol{p}^{l}(t) - \boldsymbol{p}^{inv}(t) + \boldsymbol{p}^{C}(t) - \boldsymbol{p}^{D}(t) \tag{5a}$$

$$\boldsymbol{q}(t) = \boldsymbol{q}^{l}(t) - \boldsymbol{q}^{inv}(t) \tag{5b}$$

where column vectors $\boldsymbol{p}^{l}(t)$ and $\boldsymbol{q}^{l}(t)$ are the system three-phase loads at time t, $\boldsymbol{p}^{inv}(t)$ and $\boldsymbol{q}^{inv}(t)$ represent the three-phase PV active and reactive outputs. The BESS charging and discharging power are collected in vectors $\boldsymbol{p}^{C}(t)$ and $\boldsymbol{p}^{D}(t)$. Considering the power flow model and BESS constraints listed above, the centralized BESS allocation for the hosting capacity problem can be formulated as:

$$\max \sum_{i,\phi} S_{i,\phi}^{g} \tag{6}$$

subject to: (2), (3), (4) and (5)

$$\underline{v} \le \boldsymbol{v}(t) \le \overline{v}, \forall t \tag{7a}$$

$$-\overline{q}_{i,\phi}^{inv}(t) \le q_{i,\phi}^{inv}(t) \le \overline{q}_{i,\phi}^{inv}(t), \forall i, \phi, t \tag{7b}$$

$$\overline{q}_{i,\phi}^{inv}(t) = \sqrt{1 - r(t)^2} \cdot S_{i,\phi}^{g}, \forall i, \phi, t \tag{7c}$$

$$SoC_i(T) = SoC_0, \forall i \tag{7d}$$

$$\boldsymbol{P}_{01}(t) \ge 0, \forall t \tag{7e}$$

The objective is to maximize the system total PV installed capacity. As mentioned above, both the PV inverters' reactive power outputs and the centralized BESS are considered in the hosting capacity enhancement. So, the inverters' reactive power outputs and BESS operation status can be regarded as the controllable variables. Constraints (2) to (5) and (7a) ensure that the distribution network with the centralized BESS satisfied the network constraints. Constraints (7b) and (7c) represent the PV inverters' capacity limits. SoC_0 in constraint (7d) is the initial status of BESS at the beginning of the operation circle. Constraint (7d) can ensure that the BESS will return to the initial status at the end of the operation circle and prepared for the next circle, which makes the BESS operation more practical. And (7e) is the reverse power flow constraint. It means the active power can only flow from the substation to the distributed network and no reverse power flow is allowed. The centralized BESS allocation for the hosting capacity problem is a mixed-integer linear programming problem.

D. Distributed BESS Allocation and Operation

In this subsection, the distributed BESS allocation is considered to improve the hosting capacity. For this distributed BESS allocation, the hosting capacity enhancement is achieved by optimizing the locations and status of BESSs and the reactive power outputs of PV inverters. Compared to the centralized BESS allocation, a single BESS with large capacity is replaced by a series of small BESSs in this distributed BESS allocation. The capacity of those small BESSs is equal to the capacity of the centralized one divided by the total number of small BESSs. This ensures the total capacity of BESS in the distribution network is identical in the two BESS allocations. The charging and discharging power limits proportionally change with the capacity. We also assume that at most one BESS can be allocated at buses with PV. The distributed BESS allocation for the hosting capacity problem can be formulated as:

$$\max \sum_{i,\phi} S_{i,\phi}^{g} \tag{8}$$

subject to: (2), (3c-3d), (4), (5) and (7)

$$\sum_{i} u(i) = \overline{u} \tag{9a}$$

$$0 \le p_{i,\phi}^{C}(t) \le \mu_i(t) \cdot u_i \cdot \overline{p_{i,\phi}^{C}}, \forall i, \phi, t \tag{9b}$$

$$0 \le p_{i,\phi}^{D}(t) \le \eta^{D}(1 - \mu_i(t)) \cdot u_i \cdot \overline{p_{i,\phi}^{D}} \cdot \forall i, \phi, t \tag{9c}$$

In constraint (9),$u(i)$ is a binary variable to determine whether there's a BESS installed at bus i. Constraint (9a) limits the total number of BESSs installed in the distribution network. And constraints (9b) and (9c) represent the charging and discharging power limits of BESS at bus i considering the allocation of BESSs.

III. Case Study

In this section, a benchmark case without any BESS is firstly tested on the IEEE 123-bus system [15] to calculate the maximum hosting capacity only with inverters' reactive power support. Then, the optimal centralized and distributed BESS allocations are tested on the same system. The pre-defined locations of PV are marked with red dots in Fig. 1. The daily profile of aggregate loads and PV generation are depicted in Fig.2. The centralized and distributed BESS allocations

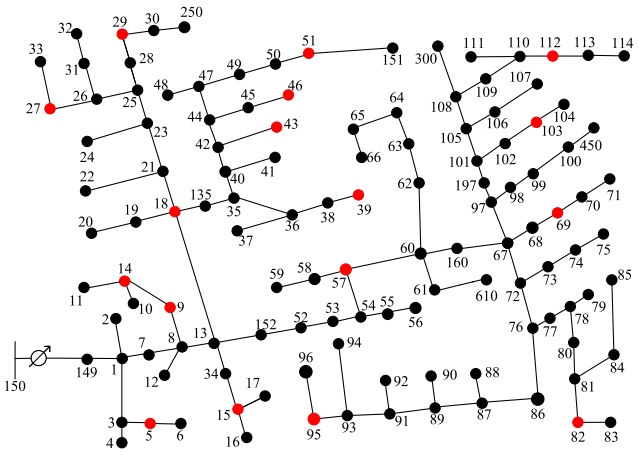

Fig. 1. IEEE 123-Bus Test Feeder

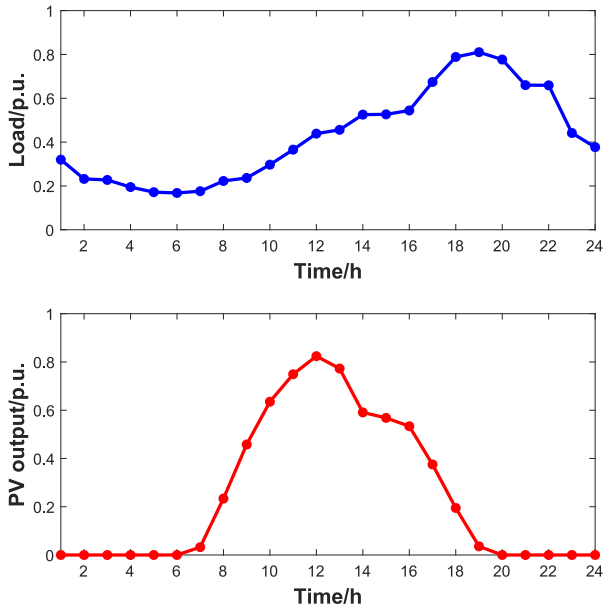

Fig. 2. Aggregate Hourly Load & loads and PV Generation

are both mixed-integer programming problems, which are performed on the Matlab 2020b platform with Yalmip toolbox and solved by Gurobi.

A. *Benchmark: Maximum Hosting Capacity without BESS*

First, the maximum hosting capacity without any BESS installed is calculated as the benchmark. Under this condition, the only device used to improve the hosting capacity is the PV inverter which can provide or absorb reactive power. The bus voltage limit is set to [0.95 1.05] p.u.. The problem can be formulated as follows:

$$\max \sum_{i,\phi} S^{g}_{i,\phi} \tag{10}$$

subject to: (2), (4), (7c) and (7e)

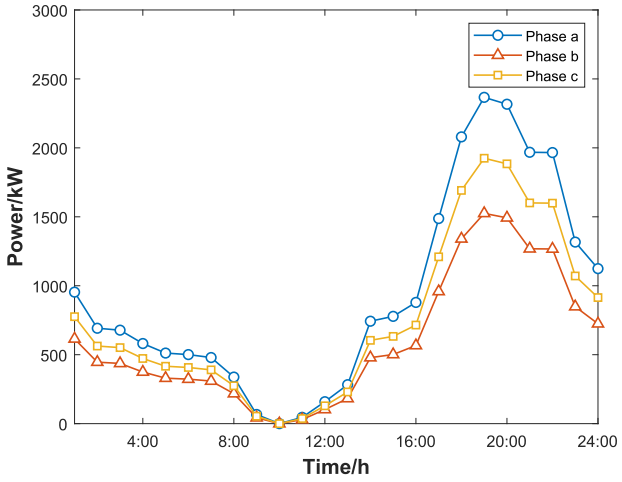

Fig. 3. Active Power Supplied by the Substation

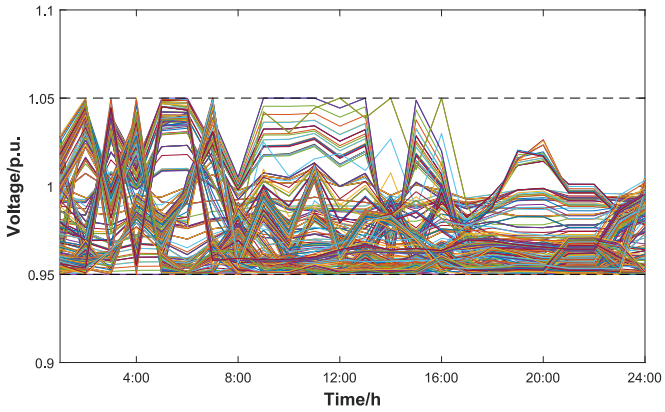

Fig. 4. The Network Voltage Profile without BESS

After solving the problem (10), the calculated maximum hosting capacity is 3,427.5 kW, and the corresponding penetration is around 18.9%. Fig. 3 and Fig. 4 show the active power supplied by the substation and the network voltage profile (each curve depicts the phase voltage magnitude fluctuation of each bus) when the maximum hosting capacity is achieved.

As can be seen in Fig. 3, at around 10 o'clock, the power flow from the substation can be as low as 0, indicating the main factor that limits the system hosting capacity is the reverse power flow constraint. If the PV capacity continues to increase, the reverse power flow may occur. That's because of the difference between the hourly load profile and the hourly PV profile. More specifically, the period with high PV generation is not coincident with the peak-load period. To avoid the reverse power flow, the system hosting capacity in this case is restricted during the period with high PV generation, which starts around 10 o'clock. And according to Fig. 4, although no voltage violation occurs, voltage magnitudes at several buses are close to the upper and lower limits. That's another obstacle that prevents system hosting capacity from increasing.

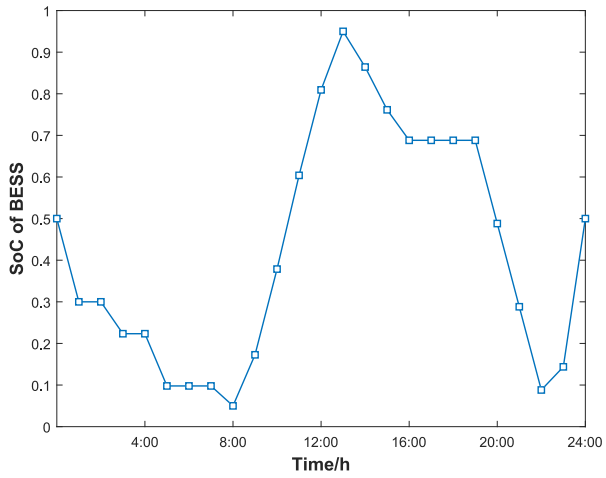

Fig. 5. SoC of the Centralized BESS

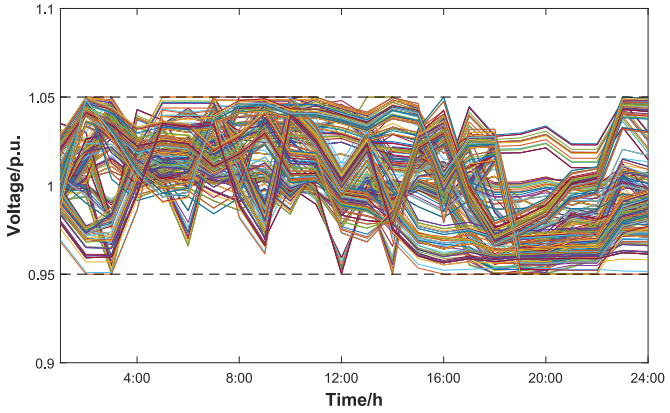

Fig. 6. The Network Voltage Profile with Centralized BESS

B. Maximum Hosting Capacity with Centralized BESS

For the centralized BESS allocation, a three-phase centralized BESS is installed near the feeder head with a capacity of 6,000 kWh. And the maximum charging power is set to 2,250 kW with the discharging and charging efficiency $\eta^D = \eta^C = 0.95$. The range of SoC is set to be [0.05 0.95] to avoid overcharging or undercharging. For the centralized BESS allocation, the hosting capacity can be increased to around 3,427.5 kW and the corresponding penetration is around 30.2%. The SoC of the centralized BESS is shown in Fig. 5 and the network voltage profile is provided in Fig. 6.

The SoC of the centralized BESS allocation decreases in the first few hours of the day, which means the BESS is in discharging status and providing power to the system. After 8 o'clock, the PV generation begins to increase and reaches its peak of the day while the load profile hasn't arrived at its peak yet. During this period, the BESS begins to work at the charging mode and store redundant power so that the SoC begins to increase. Then, as the PV generation decreases, the load gradually reaches its peak value. Meanwhile BESS provides energy back to the system, and the SoC decreases. Finally, the BESS charges again to the initial state at the end of the day for the next 24-hour circle. The voltage profiles with a centralized BESS allocation in Fig. 6 are also maintained within the predefined range. During 8 o'clock to 12 o'clock, since the BESS is charging, which means that the power are flowing to the BESS near the feeder head, the overall system voltage is high. Similarly during 22 o'clock to 24 o'clock, the system voltage rises due to the charging of BESS.

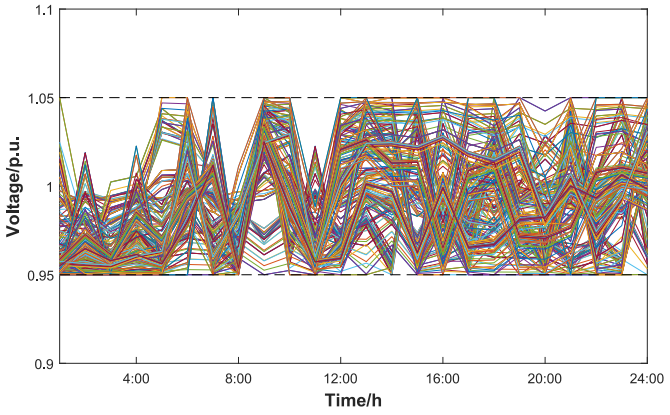

Fig. 7. The Network Voltage Profile with Distributed BESSs

C. Maximum Hosting Capacity with Distributed BESSs

In this subsection, six small BESSs, instead of one single centralized large BESS, are installed in the distribution network. Each BESS has a capacity of 1,000 kWh and the maximum charging power of 375 kW, which are equal to the capacity and charging power for the centralized BESS allocation divided by six, respectively. The range of SoC is also set to [0.05 0.95]. The buses with PV are the candidates to install the BESS, and at most one BESS can be installed on each candidate bus.

After solving the mixed-integer programming problem, the maximum system hosting capacity for the distributed BESS allocation is 5,613.4 kW. And the optimal locations of the six BESSs are presented in Table. I. And the network voltage profile is given in Fig. 7.

TABLE I
OPTIMAL LOCATIONS OF BESSS

Bus18	Bus29	Bus51	Bus57	Bus82	Bus95

Compared with the centralized BESS allocation, the distributed BESS allocation can further increase the maximum hosting capacity to be accommodated into the distribution network by 137.4 kW, which is an improvement of around 3%, and the corresponding penetration is 31 % Considering the locations of BESSs shown in Table. I, the main reason is that the BESSs are allocated throughout the system, which may avoid too large power flows concentrating to one bus.

Compared with voltage profile in Fig. 6, the the distributed BESS allocation leads to a smoother voltage profile.

TABLE II
THE MAXIMUM HOSTING CAPACITIES IN DIFFERENT CASES

BESS	No BESS	C-BESS	D-BESSs
Hosting Capacity (kW)	3427.5	5476.0	5613.4
Penetration (%)	18.9	30.2	31

Table. II gives a brief summary of the maximum hosting capacities in different cases. The results show that BESSs are beneficial to increasing the hosting capacity and the impact is significant. The distributed BESS allocation exhibits a better performance than the centralized BESS allocation.

CONCLUSIONS

This paper focuses on system hosting capacity enhancement by installing BESS. Both the centralized and distributed BESS allocations are tested on the unbalanced distribution network. The allocation and operation of BESSs are formulated as the mixed-integer programming problem to maximize the hosting capacity. The simulation results show that, with respect to the distribution network without BESS, the hosting capacity gets strictly limited by the reverse power flow constraints as well as system voltage constraints. The time-shifting ability of BESSs can be helpful to mitigate the two disadvantages and therefore increase the hosting capacity greatly. Compared with the centralized BESS allocation, the distributed BESS allocation can further improve the system hosting capacity.

REFERENCES

[1] J. Su, P. Dehghanian, M. Nazemi, and B. Wang, "Distributed wind power resources for enhanced power grid resilience," in *2019 North American Power Symposium (NAPS)*, pp. 1–6, IEEE, 2019.

[2] F. Ding and B. Mather, "On distributed PV hosting capacity estimation, sensitivity study, and improvement," *IEEE Trans. Sustain. Energy*, vol. 8, no. 3, pp. 1010–1020, Jul. 2017.

[3] S. Jothibasu, S. Santoso, and A. Dubey, "Determining PV hosting capacity without incurring grid integration cost," in *Proc. North Amer. Power Symp.*, 2016, pp. 1-5.

[4] S. S. AlKaabi, V. Khadkikar, and H. H. Zeineldin, "Incorporating PV inverter control schemes for planning active distribution networks," *IEEE Trans. Sustain. Energy*, vol. 6, no. 4, pp. 1224–1233, Oct. 2015.

[5] R. Cheng, Z. Wang, and Y. Guo, "Online voltage control for unbalanced distribution networks using projected newton method," *IEEE Trans. Power Syst*, in press, 2021.

[6] L. F. Ochoa, C. J. Dent, and G. P. Harrison, "Distribution network capacity assessment: Variable DG and active networks," *IEEE Trans. Power Syst*, vol. 25, no. 1, pp. 87–95, Feb. 2010.

[7] F. Capitanescu, L. F. Ochoa, H. Margossian, and N. D. Hatziargyriou, "Assessing the potential of network reconfiguration to improve distributed generation hosting capacity in active distribution systems," *IEEE Trans. Power Syst*, vol. 30, no. 1, pp. 346–356, Jan. 2015.

[8] L. He, Y. Liu, and J. Zhang, "Peer-to-peer energy sharing with battery storage: Energy pawn in the smart grid," *Applied Energy*, vol. 297, p. 117129, 2021.

[9] S. Gill, I. Kockar, and G. W. Ault, "Dynamic optimal power flow for active distribution networks," *IEEE Trans. Power Syst*, vol. 29, no. 1, pp. 121–131, Jan. 2014.

[10] T. Jamal, C. Carter, T. Schmidt, G. Shafiullah, M. Calais, and T. Urmee, "An energy flow simulation tool for incorporating short-term PV forecasting in a diesel-PV-battery off-grid power supply system," *Applied Energy*, vol. 254, p. 113718, 2019.

[11] P. Hasanpor Divshali and L. Söder, "Improving hosting capacity of rooftop PVs by quadratic control of an LV-central BSS," *IEEE Trans. Smart Grid*, vol. 10, no. 1, pp. 919–927, Jan. 2019.

[12] B. Wang, C. Zhang, Z. Y. Dong, and X. Li, "Improving hosting capacity of unbalanced distribution networks via robust allocation of battery energy storage systems," *IEEE Trans. Power Syst*, vol. 36, no. 3, pp. 2174–2185, May 2021.

[13] R. Cheng, L. Tesfatsion, and Z. Wang, "A multiperiod consensus-based transactive energy system for unbalanced distribution networks," *ISU Digital Repository, Iowa State Univ.,*, 2021. [Online]. Available: https://dr.lib.iastate.edu/handle/20.500.12876/104714.

[14] R. Cheng, L. Tesfatsion, and Z. Wang, "A consensus-based transactive energy design for unbalanced distribution networks," *IEEE Trans. Power Syst*, pp. 1–1, 2022.

[15] W. Kersting, "Radial distribution test feeders," *IEEE Trans. Power Syst*, vol. 6, no. 3, pp. 975–985, Aug. 1991.